

# Multifragmentation Studies in $^{84}\text{Kr}$ Interactions with Nuclear Emulsion at around 1 A GeV

V. SINGH<sup>1</sup>, S.K. TULI

Department of Physics, Banaras Hindu University, Varanasi, India

B. BHATTACHARJEE, S. SENGUPTA

Department of Physics, Gauhati University, Guwahati, India

A. MUKHOPADHYAY

Department of Physics, North Bengal University, New Jalpaiguri, India

Abstract

Projectile fragmentation of  $^{84}\text{Kr}$  in three different energy intervals has been studied. Many aspects of multifragmentation process have been examined in depth. It is observed that multifragmentation is a general low energy phenomenon associated with heavy beam. The number of Intermediate-Mass-Fragments (IMF's) shows strong projectile mass dependence.

**Keywords:** NUCLEAR REACTION Target-nucleus, photoemulsion method, fragmentation, multifragmentation, relativistic nuclear collisions.

## 1 Introduction

The interactions of relativistic nuclei with target nuclei have been studied by number of authors using several types of experimental techniques [1-2]. The nuclear emulsion technique provides a global view of the phenomena a view that can hardly be matched by other techniques which provide specific data with higher statistical significance. High energy heavy-ion collisions offer an unique opportunity to study new phase of matter. In nuclear collisions at lower beam energies ( $< 1$  A GeV), breakup of the interacting nuclei into different fragments dominates. A new kind of breakup process has been observed recently in which many fragments, each more massive than an alpha particle, are emitted in an interaction and related to the production of highly excited nuclear system [3-6]. This process is called multifragmentation because it is characterized by the production of several medium size, moderately excited fragments [7]. Many experimental and theoretical [8-11]

---

<sup>1</sup>vsingh@phys.sinica.edu.tw

studies have been done, but the underlying physics is not yet clear due to lack of experimental data. In this paper we present results obtained from an experiment in which nuclear emulsions were exposed to Krypton ( $^{84}Kr$ ) nuclei with an incident energy of 1 A GeV. We compare our results with the results of Lanthanum ( $^{139}La$ ), Gold ( $^{197}Au$ ) and Uranium ( $^{238}U$ ) at nearly the same energy.

## 2 Experimental Details

In the present experiment, we have employed a stack composed of **NIKFI BR2** nuclear emulsion pellicles of dimensions  $9.8 \times 9.8 \times 0.06 \text{ cm}^3$ , exposed horizontally to  $^{84}Kr$  ions at about 1 A GeV at the **SIS** synchrotron at **GSI**, Darmstadt (Germany). The events have been examined and analyzed with the help of a **LEITZ (ERGOLUX)** optical microscope. In order to obtain an unbiased sample of events, an along-the-track scanning technique has been employed using an oil immersion objective of 100X magnification with a digitized microscope readout. The beam tracks were picked up at a distance of 4 mm from the edge of the plate and carefully followed until they either interacted with emulsion nuclei or escaped through any one surface of the emulsion or stopped in the plate.

The interaction mean free path of  $^{84}Kr$  in nuclear emulsions has been determined and found to be  $6.76 \pm 0.21$  (1197 events) cm. The **DGKLMVT** collaboration [12] found a value of mean free path ( $\lambda$ )  $7.10 \pm 0.14$  (877 events) cm, consistent within the experimental error with our value. The classification of secondary charged particles in these events has been reported earlier [12]. As the beam passes through the emulsions, it loses its energy due to ionization and eventually stops in the nuclear emulsion. Since the beam energy decreases as beam go from the entrance edge, we have divided each plate in three major regions where the beam has energy in the range **A** (0.95 - 0.80 A GeV), **B** (0.80 - 0.50) and **C** below 0.50 A GeV (0.08 -0.50 A GeV), respectively.

In the following, we will deal only with those interactions in which at least one charged particle was produced. Example of electromagnetic dissociation of target and projectile nuclei have been rejected. The rest data samples (1100 events) in the three energy intervals contain 727, 337 and 36 events, respectively.

The charge associated with each projectile fragments has been estimated.

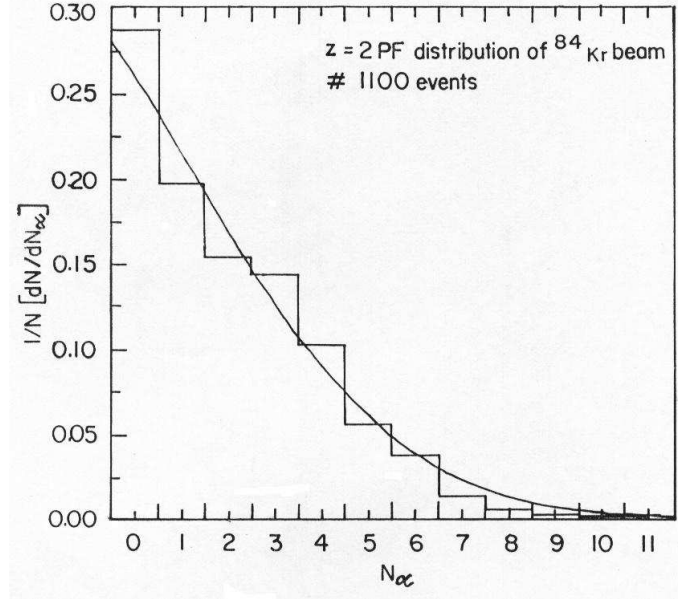


Figure 1: Frequency distribution of Alpha fragments in  $^{84}\text{Kr}$  interactions at about 1 A GeV with the Gaussian fit.

The charge of light PF's ( $Z < 10$  charge unit) has been measured by blob/gap density and by determining the gap length coefficient. For medium PF's ( $Z$  up to 19 charge unit) the charge has been determined by delta-rays ( $\delta$ ) density measurements [13]. For still heavier fragments the assignment of charge has been done by estimating the limits on charge from the range of the fragments and by comparing the fragment width relative to the beam track width [14]. The charge estimation has an accuracy of  $\pm 1$  charge unit.

### 3 Experimental Results and Discussion

The mean multiplicities of  $Z \geq 3$  projectile fragment and  $Z=2$  PF of complete set of 1100 events distributed over the entire energy range of  $^{84}\text{Kr}$  beam (950 A MeV - 80 A MeV) are  $1.21 \pm 0.04$  and  $2.03 \pm 0.06$ , respectively. The  $\langle N_f \rangle$  and  $\langle N_\alpha \rangle$  values in the above mentioned three energy intervals are  $1.17 \pm 0.05$  and  $2.02 \pm 0.08$  (interval **A**),  $1.22 \pm 0.06$  and  $2.04 \pm 0.10$  (interval **B**) and  $2.06 \pm 0.35$  and  $2.37 \pm 0.40$  (interval **C**), respectively. The multiplicity distribution of  $Z=2$  PF of  $^{84}\text{Kr}$  for complete set of minimum bias events is

Table 1:  $C_q$  moments of Z=2 PF's from  $^{84}Kr$ .

$C_q$	Energy intervals		
	A	B	C
$C_2$	$1.86 \pm 0.07$	$2.08 \pm 0.10$	$1.72 \pm 0.26$
$C_3$	$4.26 \pm 0.17$	$5.59 \pm 0.28$	$3.42 \pm 0.51$
$C_4$	$11.25 \pm 0.45$	$18.07 \pm 0.90$	$7.48 \pm 1.12$

shown in **Figure 1**. The distribution admits a Gaussian fit with a width of 8.76 and a tail extending upto 11. Events having no Z=2 PF are more probable than other type of events.

We have calculated for the alpha fragment multiplicity distribution the  $C_q$  moments ( $C_q = \langle n_\alpha^q \rangle / \langle n_\alpha \rangle^q$ ) in the minimum bias sample of interactions of  $^{84}Kr$  beam in the three energy intervals. The values are tabulated in **Table 1**. For the same order q these moments show only a weak variation with energy and no definite conclusions are possible in view of limited statistics. However there is clear variation (increase) in  $C_q$  with increasing order q of the moment.

We have plotted  $N_\alpha$  with respect to the mass number ( $A_p$ ) of the source projectile nucleus for the different minimum biased reactions at nearly similar lab energy in **Figure 2**. The data are examined to check whether the emission of alpha particles is a surface phenomenon. It is observed that alpha- multiplicity ( $N_\alpha$ ) grows slowly as  $(A_p)^{2/3}$  and the empirical relation  $\langle N_\alpha \rangle = (-0.08 \pm 0.11) \times (A_p)^{2/3}$  represents the experimental data points satisfactorily.

The maximum number and average values of the various type of projectile fragments are listed in the **Table 2**. Also included are the values for the case of gold nuclei at nearly the same energy [15].

The number of released projectile protons ( $N_p$ ) is defined from charge conservation by  $N_p = Z - (2 \times N_\alpha + \sum Z_f)$ , where  $\sum Z_f$  is the sum of charges of all  $N_f$  projectile fragments with charge  $Z_f \geq 3$  and  $N_\alpha$  is the number of alpha particles. The values listed in this table show that the average number of released projectile protons ( $N_p$ ) depends upon the energy of the projectile, and exhibits no drastic variation with the mass number of the beam. At low beam energy the projectile fragmentation does not involve a large number of singly charged products and as a result the mean value of the charge of the heaviest fragment increases. The emission of Intermediate Mass Fragments

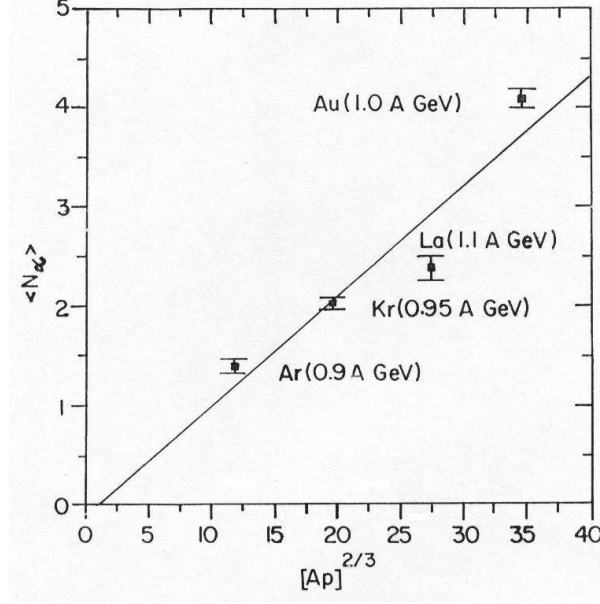


Figure 2: Plot of  $\langle N_\alpha \rangle$  Vs  $A^{2/3}$  for different projectiles at nearly similar lab energy. Solid line is the best-fit.

Table 2: Characteristics of  $^{84}\text{Kr}$  fragmentation at (0.80 - 0.95 A GeV) and (0.50 - 0.70 A GeV) and comparison with  $^{197}\text{Au}$  at (0.10 - 1.00 A GeV).

Sample	$^{84}\text{Kr}(0.80 - 0.95)\text{A GeV}$	$^{84}\text{Kr}(0.50-0.70)\text{A GeV}$	$^{197}\text{Au}(0.01-1.08)\text{A GeV}$ [15]
$N_{events}$	234	081	360
$\langle N_p \rangle$	$15.57 \pm 1.09$	$10.74 \pm 1.18$	$16.01 \pm 0.89$
$\langle N_\alpha \rangle$	$01.99 \pm 0.14$	$01.96 \pm 0.22$	$05.22 \pm 0.20$
$\langle N_f \rangle$	$01.14 \pm 0.08$	$01.22 \pm 0.13$	$02.30 \pm 0.08$
$\langle N_p^{max} \rangle$	36	36	69
$\langle N_\alpha^{max} \rangle$	08	09	15
$\langle N_f^{max} \rangle$	04	04	07
$\langle Z^{max} \rangle$	$15.43 \pm 1.08$	$20.12 \pm 2.21$	$44.47 \pm 1.36$

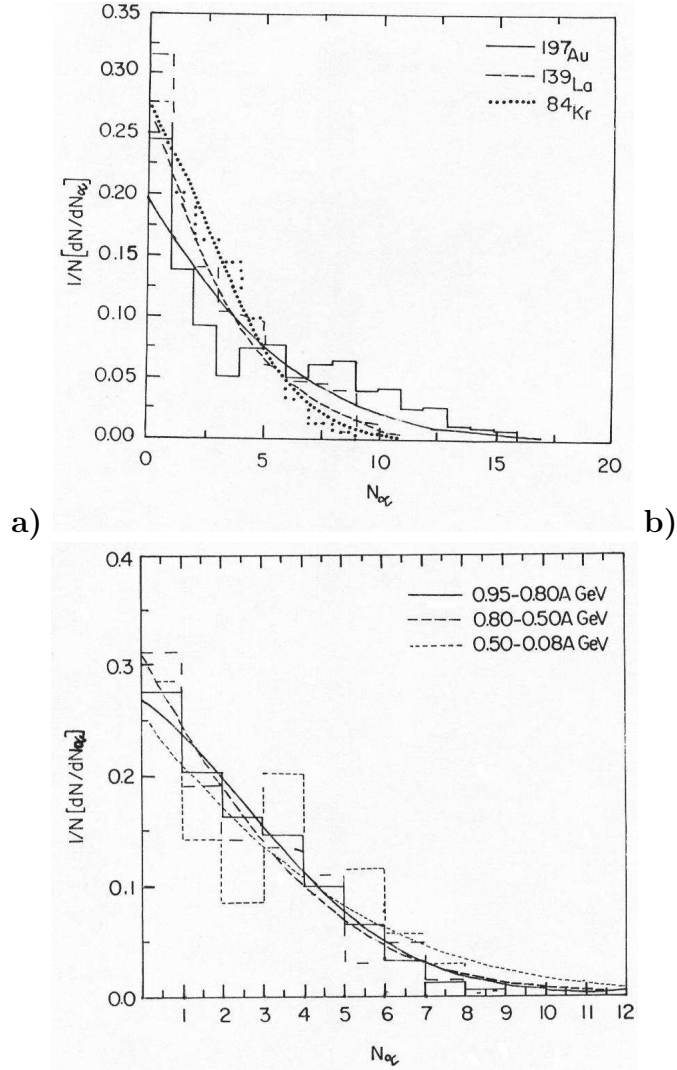


Figure 3: **(a)** Frequency distribution of alpha fragments in  $^{84}\text{Kr}$ ,  $^{139}\text{La}$  and  $^{197}\text{Au}$  interactions at 0.60 - 0.99 A GeV. Solid, dashed and dotted lines are Gaussian fits for Au, La and Kr, respectively. **(b)** Frequency distribution of alpha fragments in  $^{84}\text{Kr}$  interactions in different energy intervals. Solid, dashed and dotted lines are Gaussian fits for Kr in the mentioned energy intervals (A, B and C, respectively).

(IMF's) in case of heavy projectile is more frequent in comparison with that in case of light projectiles.

The maximum number of  $Z \geq 3$  fragments and  $Z=2$  alphas emitted is comparable at the two energies but changes when changing the projectile mass number from  $^{84}Kr$  to  $^{197}Au$ .

The fractional yield of alphas ( $Z=2$ ) from  $^{84}Kr$  at  $\sim 1$  A GeV is shown in **Figure 3(a)**, and has been fitted by a Gaussian function. For 1100 minimum biased events the maximum number of alphas in an event ( $N_{\alpha}^{max.}$ ) and the width of the distribution are found to be 11 and 7.88, respectively. The average number of alphas  $\langle N_{\alpha} \rangle$  is  $(2.0 \pm 0.06)$ . For comparison, the data from  $^{139}La + Em.$  and  $^{197}Au + Em.$  at nearly the same energy (0.60-0.99 A GeV) are also included in the figure. There is significant growth in the number of alphas with increasing projectile mass number. The width of the alpha yields from La and Au are 17.88 and 16.18, respectively.

The fractional yield of alpha particles of  $^{84}Kr$  in the three energy intervals is shown in **Figure 3(b)**. The three data sets have been fitted with the Gaussian distribution. The widths of the distributions increase with decreasing beam energy and have a magnitude of 7.88, 11.04 and 18.12, respectively. The data presented in **Figure 3(b)** show that multi-alpha emission is generally more probable at low energy [16].

The yield of  $Z \geq 3$  projectile fragments from  $^{84}Kr$  is depicted in **Figure 4(a)**, which also includes data from  $^{139}La + Em.$  and  $^{197}Au + Em.$  for comparison. These distributions have been fitted with the Gaussian function. From the  $^{84}Kr$  data it is observed that in 2% events  $N_f=0$  and at same time  $N_{\alpha}=0$  while in 12% events having  $N_f=0$  but  $N_{\alpha} \neq 0$ . Heavy beams rarely yield events having no heavier fragment. The number of events having a single ( $Z \geq 3$ ) fragment increases with decreasing beam mass number.

The frequency spectra of  $Z \geq 3$  fragments from  $^{84}Kr$  beams in the three different energy intervals together with the higher (1.4 to 1.1 A GeV) energy published data [23] are shown in **Figure 4(b)** and have been fitted by Gaussian distributions. In the total sample of 1100 events in present experiment  $\langle N_f \rangle = 1.21 \pm 0.04$ . The fitted distribution peaks at 1.6 with a width of 1.8. Notice that the maximum number of fragments in an event is four at high energy (1.4 - 1.1 A GeV) which increases to eight at low energy interval (C) marking a change in the fragmentation mode.

The probability of multifragmentation (events having two or more fragments with  $Z \geq 3$ ) in case of  $^{84}Kr$  is about 21%. It is clear from the **Figure 4(a)** that the multifragmentation increases as we go from  $^{84}Kr$  to  $^{197}Au$ .

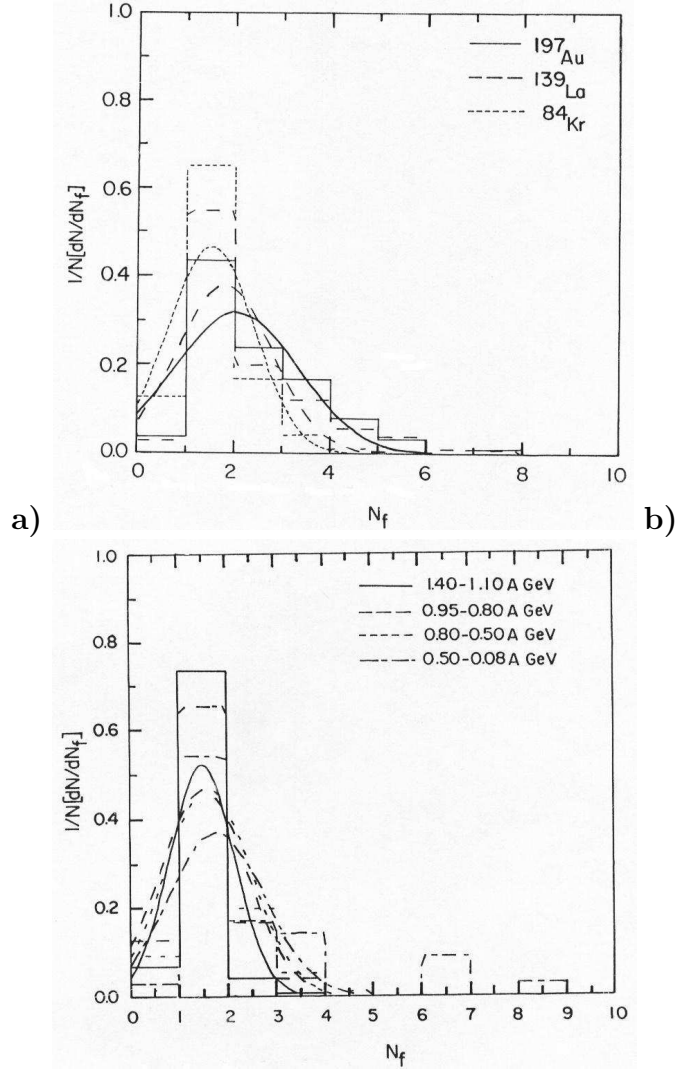


Figure 4: (a) Frequency distribution of heavier fragments ( $Z \geq 3$ ) from different beams at 0.60 - 0.99 A GeV together with the Gaussian fit. (b) Frequency distribution of heavier fragments ( $Z \geq 3$ ) from  $^{84}\text{Kr}$  interactions in different energy intervals together with the Gaussian fit.



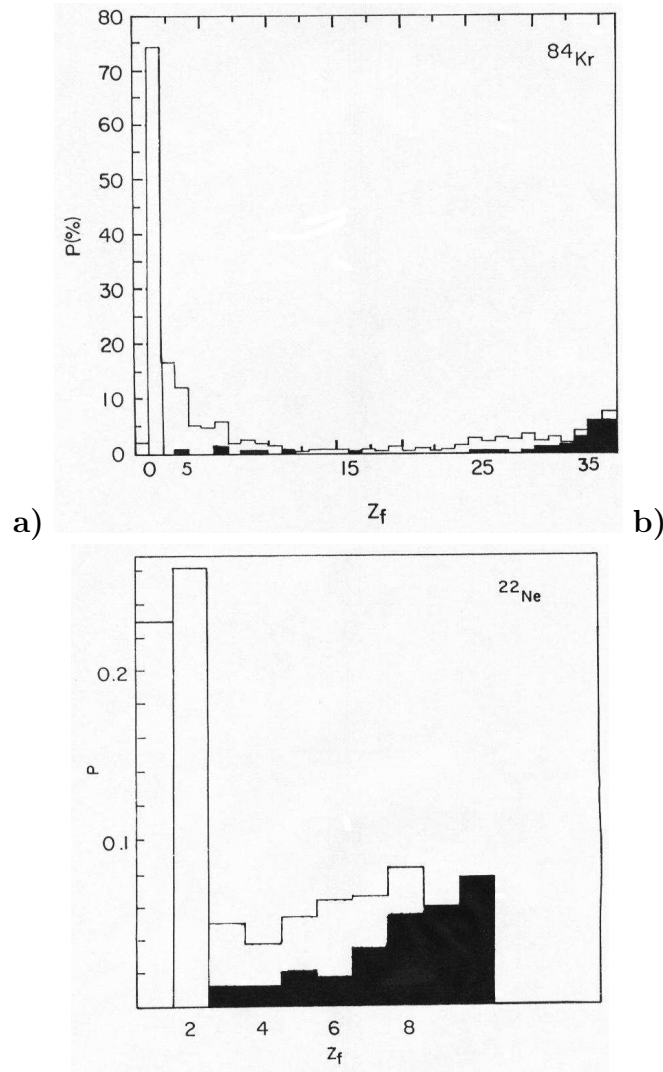


Figure 5: The probability of fragments of (a)  $^{84}\text{Kr}$  and (b)  $^{22}\text{Ne}$  projectiles into fragments with charge  $Z_f$ . Solid area represents the probability for a given fragment  $Z_f$  not to be accompanied by alpha particle(s).  $Z_f=1$  denotes events without alpha particle(s) or heavier fragment(s).

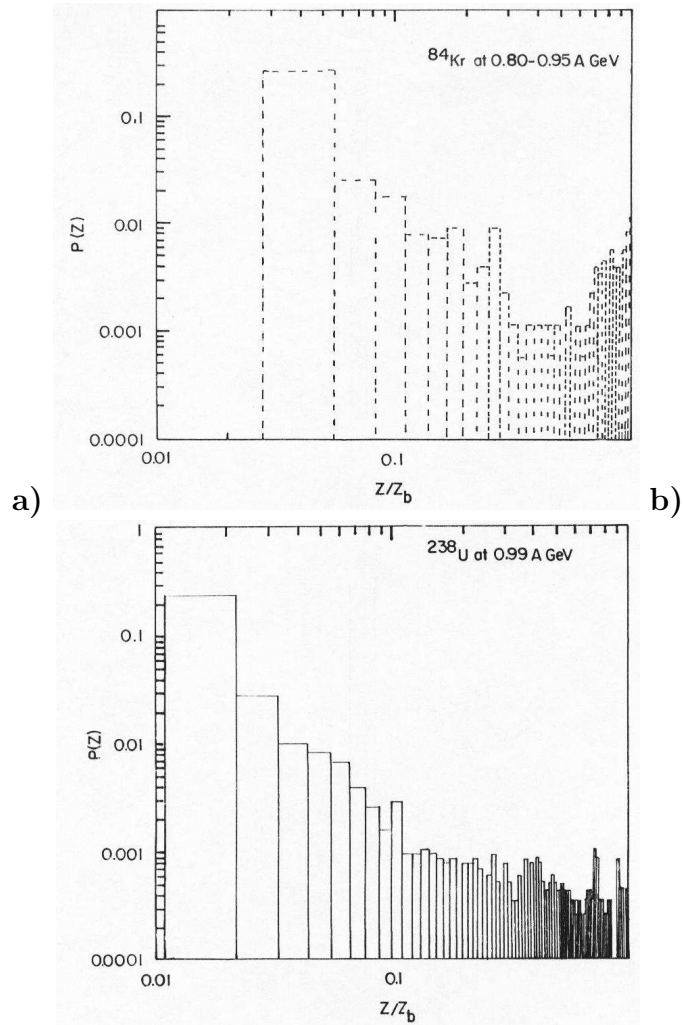
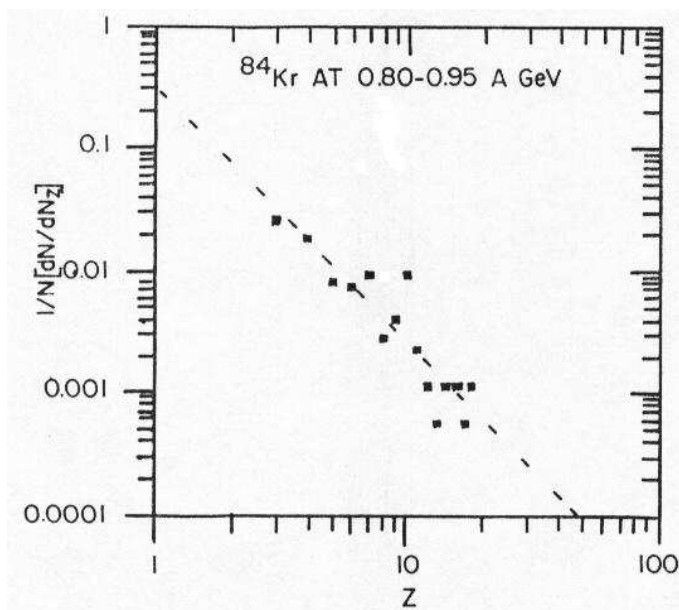
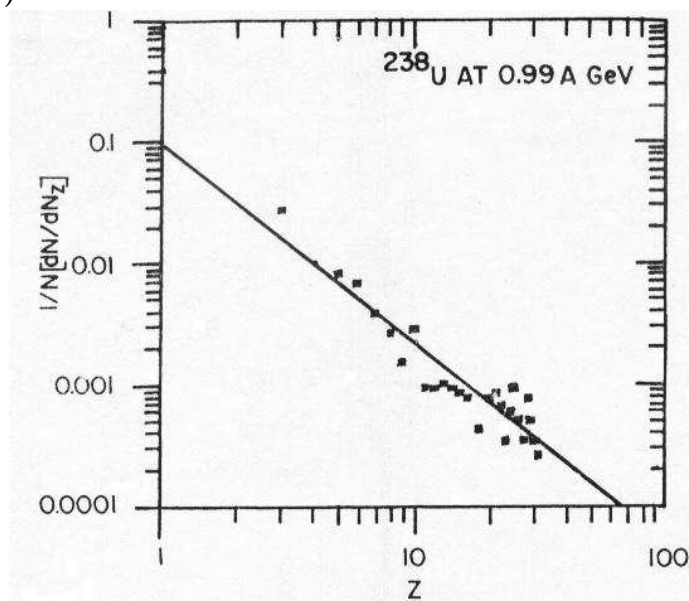


Figure 6: The probability of fragment charge normalised to the beam charge in (a)  $^{84}\text{Kr}+\text{Em.}$  and (b)  $^{238}\text{U}+\text{Em.}$  events at  $\sim 1$  A GeV.



a)

b)



c)

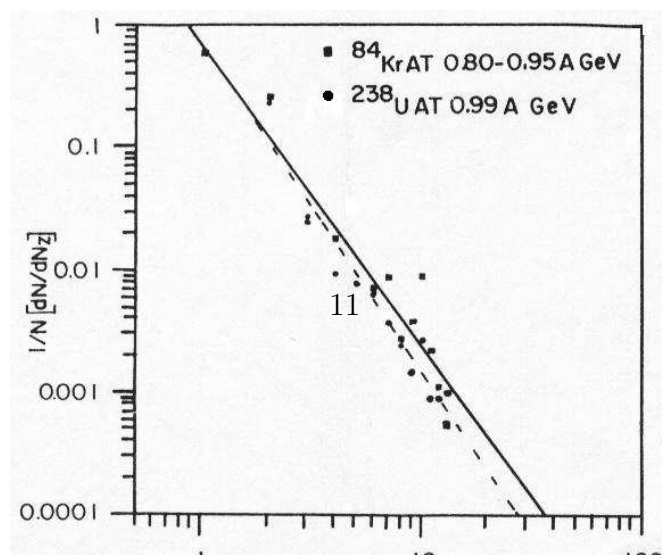


Table 3: Gaussian distribution parameters for  $^{84}\text{Kr}+\text{Em.}$  in different beam energy intervals.

Energy (A GeV)	Center	Width
1.46 - 1.10	1.48	1.33
0.95 - 0.80	1.52	1.78
0.80 - 0.50	1.60	1.76
0.50 - 0.08	1.77	1.96

In other words the multifragmentation is a more common phenomenon in heavier mass beams. A Gaussian shape fit has been made to the multiplicity distributions of projectile fragments. The width in these fits are broader for heavier mass beam and center of these distributions are shifted towards higher  $N_f$ . These observations are consistent with the features expected in multifragmentation process.

The Gaussian distribution parameters obtained in different beam energy intervals are summarised in **Table 3**. One can conclude from this table that with increasing beam energy the width of the distribution decreases and the location of the peak shifts to lower  $N_f$  values. The tail of the distribution extends further for low beam energy. This indicates that the energy is more uniformly distributed over a large cross-sectional area in low beam energy showing that the multifragmentation is primarily a low beam energy phenomenon.

We have already reported the data on projectile fragmentation for  $^{84}\text{Kr}$  as a function of beam energy [17-19] and have observed that the number of PF's with charge one & two increases with increasing beam energy. But at CERN energy, data on PF's from  $^{16}\text{O}$  show that the yield of fragments ( $Z \geq 3$ ) increases significantly as the beam energy increases [20].

The probability distribution of heavy projectile fragments and alpha particles emitted from  $^{84}\text{Kr}$  at around 1 A GeV beam energy is presented in **Figure 5(a)**. For comparison with this data, we have included a large data set of interactions of  $^{22}\text{Ne}$  nuclei with an energy of 4.2 A GeV in **Figure 5(b)** [21].

We have tabulated some important parameters describing the projectile fragmentation of  $^{84}\text{Kr}$  and compared with the data of  $^{22}\text{Ne}$  at 4.2 GeV/nucleon in **Table 4**. From this table a number of observations are possible.

Table 4: Some parameters describing the projectile fragmentation for inelastic interactions of  $^{22}\text{Ne}$  [20] and  $^{84}\text{Kr}$  in emulsion.

Fragmentation Mode	$^{22}\text{Ne}(4.2)$	$^{84}\text{Kr}(0.95-0.80)$	$^{84}\text{Kr}(0.80-0.08)$
	A GeV	A GeV	A GeV
	Probability (in percents)	for different	fragmentation
	modes		
Two fragments with $Z \geq 3$	$1.0 \pm 0.2$	$16.78 \pm 0.67$	$18.01 \pm 0.90$
One fragments with $Z \geq 3$	$50 \pm 1$	$65.06 \pm 2.60$	$36.02 \pm 1.80$
Fragment(s) with $Z \geq 3$	$29 \pm 1$	$26.13 \pm 1.05$	$29.84 \pm 1.49$
and no alpha particle			
Fragment(s) with $Z \geq 3$	$21 \pm 1$	$61.21 \pm 2.45$	$61.56 \pm 3.08$
and alpha particle(s)			
Alpha particles and no	$26 \pm 1$	$11.28 \pm 0.45$	$5.43 \pm 0.34$
heavier fragments			
No multiply charged	$23 \pm 1$	$1.38 \pm 0.06$	$2.15 \pm 0.11$
fragment			
	Mean number of	multicharge	fragments per
	event		
Fragments with $Z \geq 3$	$0.50 \pm 0.01$	$1.05 \pm 0.04$	$1.02 \pm 0.05$
Alpha particles	$0.72 \pm 0.01$	$2.98 \pm 0.12$	$3.35 \pm 0.17$
	Mean charge of	the fragment	
Fragments with $Z \geq 3$	$7.8 \pm 0.1$	$14.48 \pm 0.87$	$17.53 \pm 1.75$
and no alpha particles			
Fragments with $Z \geq 3$	$5.4 \pm 0.1$	$06.53 \pm 0.26$	$07.96 \pm 0.48$
and alpha particle(s)			

The probability of producing one and two fragments is strongly dependent on beam mass number. An increase in the probability of producing fragment(s) is observed as the mass of the projectile increases. The probability of producing fragment(s) with no accompanying alpha particles is independent of mass and energy of the beam.

The probability of fragmentation of projectile into alpha particle(s) shows strong dependence on the mass of the beam and is independent of energy. The probability that only alpha particles but no heavier fragments are produced decreases with increasing mass of the projectile. The low and high energy  $^{84}\text{Kr}$  data have a strong dependence on the energy of the beam i.e., probability of producing only alpha particles increases with increasing beam energy. There is a rapid decrease in the number of events with no multiple charged fragments, as the mass of the projectile increase.

The mean number of fragments and alpha particles as well as the mean charge of the fragments all increase with increasing mass of the projectile. The probability of producing multiple fragments with  $Z \geq 3$  increases rapidly with increasing mass of the projectile. The mean charge of the fragments with no accompanying alpha particles shows rapid increase with increasing mass of the beam. A similar feature can be observed in fragments with alpha particles fragmentation mode, which is consistent with the interactions of low energy  $^{197}\text{Au}$  nuclei in emulsions [22].

In the strict thermodynamic sense phase transitions are only defined for infinite system. In nature there are a few mesoscopic system with numbers of constituents on the order of  $10^2$  to  $10^5$ . Fragmentation of atomic nuclei is a system where we expect to experience phase transitions under certain conditions and for which mesoscopic finite-size effect should play very important roles. For now more than two decades, there have been speculations that we may be able to see a first-order phase transition between the Fermi liquid of ground state nuclei and the hadronic gas phase of individual nucleons and / or small clusters [23]. One interesting thing is that this first-order transition will terminate at a critical point, where the transition becomes continuous and critical exponents of nuclear matter can be determined experimentally following the so-called Fisher droplet model [24]. In this context, particular attention must be focus on the power-law dependence of the yield of nuclear fragments as a function of mass number.

The charge distribution of projectile fragments from  $^{84}\text{Kr}$  interactions is shown in **Figure 6(a)** and the corresponding distribution from  $^{238}\text{U}$  is included as **Figure 6(b)** for comparison. The figure shows as increase in the

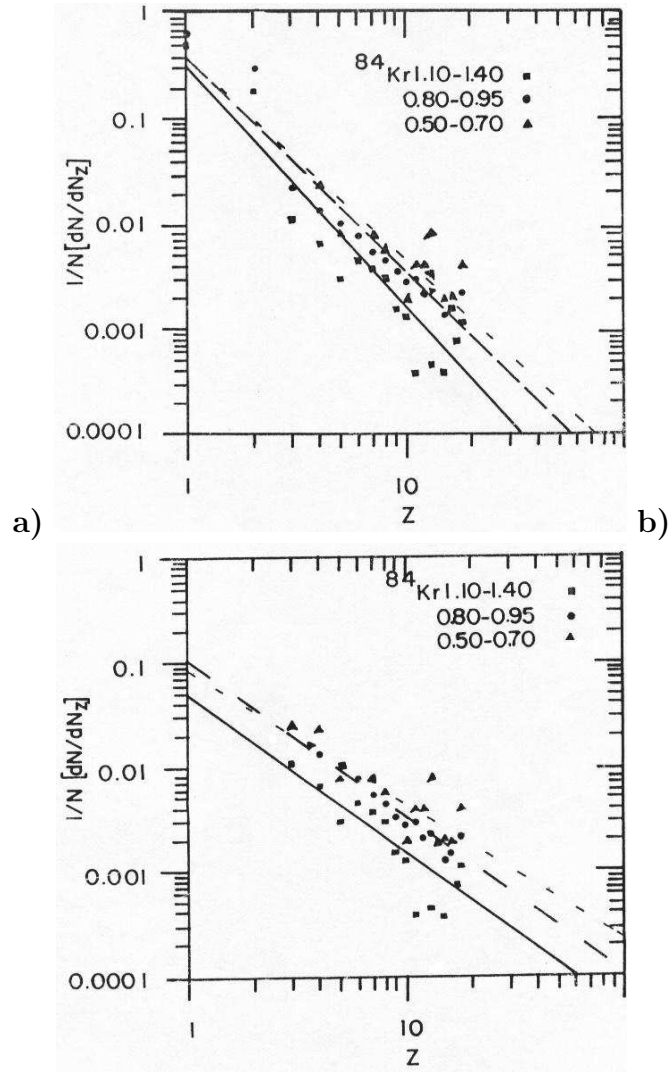


Figure 8: The charge of the projectile fragment fitted with the linear function (a) from 1 to  $Z_{b/2}$  and (b) from 3 to  $Z_{b/2}$  for  $^{84}\text{Kr}$  in energy intervals 1.1 - 1.4, A and 0.50 - 0.70 A GeV.

Table 5: The value of the exponent for different beams at nearly same ( $\sim 1.0$  A GeV) energy.

Beam	Z from 1 to $Z_{b/2}$ Exponent	Z from 3 to $Z_{b/2}$ Exponent
$^{238}\text{U}$	$-(2.67 \pm 0.12)^*$	$-(1.66 \pm 0.07)$
$^{197}\text{Au}$	$-(2.55 \pm 0.08)$	$-(1.56 \pm 0.05)$
$^{84}\text{Kr}$	$-(2.45 \pm 0.16)$	$-(1.49 \pm 0.09)$

\* The exponent ( $\tau$ ) is  $-(2.01 \pm 0.09)$  up to  $Z=25$  [27]

Table 6: The value of the exponent of  $^{84}\text{Kr}$  beam in different energy intervals.

Energy (A GeV)	Z from 1 to $Z_{b/2}$ Exponent	Z from 3 to $Z_{b/2}$ Exponent
0.84 - 1.52	$-(2.29 \pm 0.09)^*$	$-(1.50 \pm 0.06)$
0.80 - 0.95	$-(2.05 \pm 0.13)$	$-(1.49 \pm 0.09)$
0.50 - 0.70	$-(1.90 \pm 0.21)$	$-(1.27 \pm 0.14)$

\* The exponent ( $\tau$ ) is  $-(2.91 \pm 0.11)$  up to  $Z=11$  [28]

yield of low charge PF's in heavier beams. This indicates a greater degree of breakup for heavier beams [25]. To facilitate inter comparison of fragment spectrum from beams of different charge we choose to show the distribution as a function of the charge of the fragment divided by the beam charge. Clearly, in case of  $^{84}\text{Kr}$  we can see the U-shaped mass yield spectra and the power-law dependence of the yield of the low-to heavier mass fragments upto the mass.

The charge distribution of all the projectile fragments produced in our interactions are shown in the **Figure 7(a)**. An inverse power law given by  $f(Z) \propto Z^\tau$  reproduces the major features of this distribution remarkably well. The charge spectrum from  $Z=3$  up to the  $Z_b/2$  has been fitted with the above function and compared with  $^{238}\text{U}$  in **Figure 7(b)**. **Figure 7(c)** represents the data for  $^{84}\text{Kr}$  and  $^{238}\text{U}$  from  $Z=1$  to  $Z_b/2$ . The values of the exponents for  $^{84}\text{Kr}$  are  $-2.45 \pm 0.16$  and  $-1.49 \pm 0.09$  for charges 1 to  $Z_b/2$  and 3 to  $Z_b/2$ , respectively. Notice, this simple trend is not exhibited by PF of excessively large charge [26]. The rise in the yield of heavier fragments is due to the events in which only a single heavy fragment  $Z \geq 3$  is emitted.

To compare the results from different beams at the same energy and those from  $^{84}\text{Kr}$  beam in different energy intervals we summarise the fit parameters



in **Tables 5 and 6**. On examining the data from different beams at nearly the same beam energy, it is found that the values of the exponent increase weakly with increasing mass of the projectile. This holds also for the fit from 3 to  $Z_b/2$ . It shows that the emission of intermediate mass fragment (**IMF**) increases with increasing the mass of the projectile.

The values of the exponent at different beam energies of  $^{84}Kr$ , as plotted in **Figure 8 (a and b)**, tabulated in **Table 6**, show an increasing trend with beam energy. An increase in the slope of the fitted straight lines with increasing beam energy has earlier been reported [15] .

An inverse power law dependence of mass yield has been interpreted as a signature for the occurrence of statistical clustering expected in the liquid - gas phase near its critical point [29,24] and this power - law is similar to the droplet size distribution close to the critical temperature in the Fisher's theory of condensation [30]. Power - law behaviors have also been seen in cluster - size distributions at the percolation threshold [31,32]. Such a power - law shows the validity of a liquid - gas phase transition at a critical temperature.

## 4 Conclusions

The following conclusions have been drawn from the results of the present work and the subsequent analysis.

The  $\langle N_p \rangle$  is strongly dependent on the energy of the projectile. It is a good measure of the total excitation energy introduced in the system. The average value of the charge carried by the heaviest projectile fragment in an event is more at low projectile energy. The number of IMF's shows strong projectile mass dependence.

There is a systematic increase in  $\langle N_\alpha \rangle$  and  $\langle N_f \rangle$  with the increase in projectile mass.

Observations indicate that the multifragmentation is a more common phenomenon in heavier mass beams and at lower beam energy. The energy distribution over large volume is more uniform at low beam energy.

The charge distribution of projectile fragments shows an inverse power law [  $f(Z) \propto Z^\tau$  ] behaviour. At the same energy, the heavier beams undergo greater degree of breakup. Power - law dependence is consistent with the validity of liquid - gas phase transition at this energy.

## 5 Acknowledgments

Partial support from DAE (Department of Atomic Energy) and UGC (University Grant Commission), Govt. of India for carrying out this work is gratefully acknowledged.

## References

- [1] J. Bartke, Int. Journ. of Mod. Phys. **A4** 1319 (1989).
- [2] J.P. Blaziot et al., Nucl. Phys. **A525** 479c (1991).
- [3] Y.D. Kim et al., Phys. Rev. Lett. **63** 494 (1989).
- [4] Y. Blumenfeld et al., Phys. Rev. Lett. **66** 576 (1991).
- [5] E. Piasecki et al., Phys. Rev. Lett. **66** 1291 (1991);  
D.R. Bowman et al., *ibid.* **67** 1527 (1991).
- [6] B. Jakobsson et al., Nucl. Phys. **A509** 195 (1990);  
S.J. Yennello et al., Phys. Rev. Lett. **67** 671 (1991);  
S.J. Yennello et al., Phys. Lett. **B246** 26 (1990).
- [7] B. Jakobsson, Aug.10-15, Invited talk presented at the 6th. Nordita Meeting on Nuclear Physics, Kopervik, Norway (1989).
- [8] D.H.E. Gross, Rep. Prog. Phys., **53** 605 (1990).
- [9] W. Lynch, Annu. Rev. Nucl. Part. Sci. **37** 493 (1987).
- [10] W.A. Friedman, Phys. Rev. **C42** 667 (1990).
- [11] G. Bersch and P.J. Siemens, Phys. Lett. **B126** 9 (1983).
- [12] S.A. Krasnov et al., Czech. J. of Phys. **46** 531 (1996).
- [13] A.Z.M. Ismail et al., Phys. Rev. Lett. **52** 1280 (1984).
- [14] P.L. Jain et al., Phys. Rev. **C44** 844 (1991).
- [15] M.L. Cherry et al., Phys. Rev. **C53** 1532 (1996).

- [16] R. Holynski, Nucl. Phys. **A566** 191 (1994).
- [17] N.P. Andreeva et al., Yad. Fiz. **47** 157 (1988).
- [18] V. Singh et al., Presented in Int. Conf. on High Energy Physics, Kracow, Poland (1996)
- [19] V. Singh et al., Presented in National Symposium on Nuclear Physics, Pantnagar, India, 288 (1996).
- [20] C.J. Waddington et al., 21st ICRC Conference papers, Adelaide, Australia, 8, 87 (1990).
- [21] C.J. Waddington and P.S. Frier, Phys. Rev **C52** 888 (1985).
- [22] L.Y. Geer et al., Phys. Rev. **C52** 334 (1995).
- [23] A.D. Panagioutou et al., Phys. Rev. Lett. **52** 496 (1984);  
A.L. Goodman et al., Phys. Rev. **C30** 851 (1984);  
D.H.E. Gross, Nucl. Phys. **A428** 313c (1984).
- [24] M.E. Fisher, Physica **3** 255 (1967).
- [25] P.L. Jain et al., Phys. Rev. Lett. **68** 1656 (1992).
- [26] V. Singh et al., XII DAE Symposium on High Energy Physics, Guwahati, India, 19 (1997)
- [27] P.L. Jain et al., Phys. Rev. **C46** 10 (1992).
- [28] P.L. Siemens, Nature **305** 458 (1982);  
J. Pochodzalla et al., Phys. Rev. Lett. **75** 1040 (1995);  
Y.-G. Ma et al., Phys. Lett. **B390** 41 (1997).
- [29] J.E. Finn et al., Phys. Rev. Lett. **49** 1321 (1982).
- [30] D. Stauffer, Phys. Rev. **54** 1 (1979).
- [31] L.G. Moretto et al., Annu. Rev. Nucl. Part. Sci. **43** 397 (1990);  
L.G. Moretto et al., Nucl. Phys. **A523** 651 (1991);  
J. Aichelin, Phys. Rep. **202** 235 (1991);  
D. Stauffer, Phys. Rep. **54** 1 (1979).

- [32] X. Campi, Phys. Lett. **B208** 351 (1988);  
W. Baur and A. Botvina, Phys. Rev. **C52** 1750 (1995).